C.P. No. 1189

MINISTRY OF DEFENCE (PROCUREMENT EXECUTIVE)

AERONAUTICAL RESEARCH COUNCIL

CURRENT PAPERS

The Effect of Conical Thickness Distributions on the Separated Flow past Slender Delta Wings

By

H. Portnoy,
University of Salford
and
S. C. Russell,
Crane Ltd., Stockport

Communicated by J. H. B. Smith, RAE

LONDON· HER MAJESTY'S STATIONERY OFFICE

1971

Price 48½p net

C.P. No.1189**
April, 1971

The Effect of Small Conical Thickness Distributions on the Separated Flow past Slender Delta Wings

- By -
H. Portnoy,
University of Salford
and
S. C. Russell,
Crane Ltd., Stockport*

Communicated by J. H. B. Smith, RAE

SUMMARY

A method is described for calculating the first order effects of a small, conical thickness distribution on the separated flow past uncambered, slender delta wings. An extension to the case of small camber is possible, but this is not done here.

The flow model utilised is that of Brown and Michael[2], but the technique could be applied using more sophisticated representations of the vortex sheets from the leading edges.

Results are presented giving the vortex-core positions and normal-force coefficient curves for several wings with thin, rhombic cross-sections of various thickness ratios.

Comparison with a limited number of experimental results indicates that although the theory is subject to the basic inaccuracies inherent in the Brown and Michael treatment, some of the changes due to thickness predicted are fairly good. Thus, the spanwise shift of the vortex due to thickness at a given incidence and the change of normal-force coefficient due to thickness are predicted fairly well, whereas the vertical core movements calculated are very poor. Pressure distributions have been calculated[10] but these are not presented here as they exhibit similar unrealistic features to those calculated by Brown and Michael[2] for zero thickness.

---

*Formerly with AEI, Manchester.

**Replaces A.R.C.32 834

1. Introduction

The calculation of the separated flow past thin, uncambered, slender, delta wings at zero yaw has been considered by several authors using mathematical models of the flow which vary in complexity (Refs. 1 to 4). All these authors assume conical flow; that is, constant flow parameters along straight lines through the wing apex, since, for a slender uncambered, delta wing, this assumption is compatible with the wing geometry, except very close to the trailing edge at subsonic speeds. Non-conical effects and camber on thin wings have been considered in Refs. 5 and 6.

Smith[7] has considered a conical delta wing with rhombic cross sections. He uses the sophisticated flow model of Ref. 4 and treats the cross-sectional effects by use of an exact transformation making no assumption of small thickness/span ratio.

The present note develops a method of finding the effects of conical thickness distributions on wings with small thickness/span ratios and sharp leading edges but otherwise of any shape. The method could be extended to include the effects of small camber but this has not been done here. The flow model used is that of Brown and Michael[2], although the technique could be used with the more sophisticated models. The Brown and Michael method replaces each rolled up vortex core by a single, concentrated point vortex, and each feeding sheet by a cut in the two-dimensional, cross-flow field, which connects the isolated vortex and the leading edge, thereby rendering the potential single valued. The conditions which are then applied to determine the isolated vortex strength and position are that the flow separates from the leading edge and that the sum of the forces on the feeding sheet and the concentrated vortex should be zero. Despite the shortcomings of the Brown and Michael results it is hoped that the present work will be adequate for predicting some of the perturbations of the wing properties due to small thickness, so that these could then be used together with more accurate results for the-zero thickness-wing case, such as those of Ref. 4.

Notation/

Notation

A_0	see equation (41).
A_1	see equation (41).
A_2	see equation (41).
A_3	see equation (41).
$b_0(x)$	function of cross-sectional area distribution and Mach number appearing in the slender-body potential.
C_N	normal-force coefficient.
$f\left(\frac{\sigma}{x}\right)$	any function of $\frac{\sigma}{x}$.
$h(\sigma)$	see equations (18) to (20).
K	tangent of wing apex semi-angle.
$m(y_1)$	source strength on cut in σ_1 plane. See equation (26).
r	$\sqrt{x^2+y^2}$.
$S(x)$	wing cross-sectional area at $x = x$.
$S'(x)$	derivative of wing cross-sectional area at $x = x$.
s	value of y at position of wing edge. Wing semi-span at x.
s_1	value of y_1 at position of wing edge.
T	wing thickness function. See equation (2).
t	centre-line half-thickness at station x.
U	free-stream speed.
$W(\sigma)$	complex potential such that $\phi_h = \mathrm{Re}\, W(\sigma)$.
$W_0(\sigma)$	W at zero incidence

$W_1(\sigma)$ /

$W_1(\sigma)$	see equation (17)
$w(\sigma)$	part of $W(\sigma)$ due to incidence.
x,y,z	Cartesian "body" co-ordinates.
y_0	real part of σ_0 .
y_1	real part of σ_1 .
y'	integration variable corresponding to y.
y_1'	integration variable corresponding to y_1.
Z_0	imaginary part of σ_0 .
Z_1	imaginary part of σ_1 .
α	wing incidence.
γ	strength of vortex on right-hand side.
ϵ	thickness parameter = t/s.
η	integration variable corresponding to y/s.
ν	normal to wing cross-section in a plane x = constant.
ρ	density of free stream.
σ	= $y + iz$.
σ_0	value of σ at vortex on right-hand side.
σ_1	complex variable defined by transformation (18).
σ_{0_1}	transformed value of σ_0 in σ_1 plane.
ϕ	perturbation potential.
ϕ_h	part of slender-body potential. See equation (6).
ϕ_{h_1}	= Re $\Omega(\sigma_1)$.

$\Omega(\sigma_1)$/

$\Omega(\sigma_1)$ value of $W(\sigma)$ in σ_1 plane.

$\Omega_0(\sigma_1)$ value of $W_0(\sigma)$ in σ_1 plane.

$\omega(\sigma_1)$ value of $w(\sigma)$ in σ_1 plane.

---

2. Formulation of the Problem

Consider a low-aspect-ratio uncambered delta wing, as shown in Fig. 1, having a conical thickness distribution symmetrical about its mean plane.

Let Ox, Oy and Oz be a right-handed system of body axes with origin at the wing apex, such that the x-y plane coincides with the wing mean plane. Ox lies along the wing centre-line pointing towards the trailing edge and Oy points to the starboard side. The oncoming air-stream, with speed U and density ρ, is at incidence α to the mean plane and is parallel to the z-x plane.

If the wing has a semi-apex angle $\tan^{-1}K$ and its centre-line half-thickness and semi-span at distance x from the apex are t and s respectively, then we may define a thickness parameter ε by the equation

$$t = \varepsilon s = K\varepsilon x . \qquad \cdots (1)$$

For a slender wing, $K \ll 1$ and for a wing which is also <u>thin</u> $\varepsilon \ll 1$ as well. The incidence α is $O(K)$ (or less).

The conical form of the wing upper and lower surfaces may now be defined by the equation

$$z = \pm t\, T\left(\frac{y}{s}\right) = \pm K\varepsilon x\, T\left(\frac{y}{Kx}\right) , \qquad \cdots (2)$$

where T is a general thickness function which must satisfy the relationships

$$\left.\begin{aligned} &T(\pm 1) = 0 \qquad \text{and} \quad |T'(\pm 1)| \neq \infty \\ &\text{for sharp edges. We will assume port and starboard} \\ &\text{symmetry, so that} \\ &T\left(\frac{y}{s}\right) = T\left(-\frac{y}{s}\right) \qquad \text{and} \quad T'\left(\frac{y}{s}\right) = -T'\left(-\frac{y}{s}\right) . \end{aligned}\right\} \qquad \cdots (3)$$

We/

We now define a perturbation potential ϕ such that the complete potential is equal to

$$(U \cos \alpha)\, x + \phi. \qquad \cdots (4)$$

Thus, at great distances from the wing

$$\frac{\partial \phi}{\partial z} \to U \sin \alpha$$

or, for small α,

$$\frac{\partial \phi}{\partial z} \to U\alpha + O(\alpha^3). \qquad \cdots (5)$$

ϕ satisfies the usual linearised equation for compressible flow and for the case of a slender wing we may make the well known slender-body approximations[8]* so that ϕ is found to be a solution of Laplace's equation in the two dimensions y and z, with the co-ordinate x only entering as a parameter through the boundary conditions. From the general, slender-body solution[8] we may write

$$\phi = \phi_h + b_o(x), \qquad \cdots (6)$$

where b_o is a function of cross-sectional area and Mach number only, given in Ref. 8 and where the behaviour of the harmonic function ϕ_h for large $r = \sqrt{z^2 + y^2}$ is given by

$$\lim_{r \to \infty} \left(\phi_h - U\alpha z - \frac{US'(x)}{2\pi} \log r \right) = 0. \qquad \cdots (7)$$

$S'(x)$ is the wing cross-sectional area derivative so that, in this case,

$$\begin{aligned} S'(x) &= 2 \frac{\partial}{\partial x} \int_{-s}^{s} t\, T\left(\frac{y}{s}\right) dy \\ &= 2 \frac{\partial}{\partial x} K^2 \epsilon x^2 \int_{-1}^{1} T(\eta)\, d\eta \\ &= 4 \epsilon K^2 x \int_{-1}^{1} T(\eta)\, d\eta. \end{aligned} \qquad \cdots (8)$$

Since/

*Note that ϕ as defined by (4) is not the same perturbation potential as that used in Ref. 8. The latter is equal to $\phi - (U \sin \alpha) z$ in the present notation.

Since ϕ_h, like ϕ, is a harmonic function of y and z we can write

$$\phi_h = \mathrm{Re}\, W(\sigma) , \qquad \cdots (9)$$

where

$$\sigma = y + iz . \qquad \cdots (10)$$

The complex function W can depend on x through the boundary conditions and in view of the conical nature of the flow it must be of the form

$$W = x f\left(\frac{\sigma}{x}\right) . \qquad \cdots (11)$$

It follows that

$$\frac{\partial W}{\partial x} = \frac{W}{x} - \frac{\sigma}{x}\frac{\partial W}{\partial \sigma}$$

$$= \frac{K}{s}\left(W - \sigma \frac{\partial W}{\partial \sigma}\right) . \qquad \cdots (12)$$

If ν is the normal to a cross-section of the wing by a plane x = constant, the wing surface tangency condition is that, at a point on the surface,

$$\frac{\partial \phi}{\partial \nu} = \left(U \cos \alpha + \frac{\partial \phi}{\partial x}\right)\frac{d\nu}{dx} , \qquad \cdots (13)$$

where $\frac{d\nu}{dx}$ is the tangent of the angle between the local tangent plane and the positive x axis. It can be shown that, on both the upper and lower wing surfaces,

$$\frac{d\nu}{dx} = \frac{\varepsilon\,(KT - y/x\, T')}{\sqrt{1 + \varepsilon^2 T'^2}} . \qquad \cdots (14)$$

If α is small and the perturbation velocities are very much less than U then, using (6) and (14), equation (13) becomes

$$\frac{\partial \phi_h}{\partial \nu} = \frac{U\varepsilon\,(KT - y/x\, T')}{\sqrt{1 + \varepsilon^2 T'^2}}$$

$$= U\varepsilon\,(KT - y/x\, T') + O(K\varepsilon^3) , \qquad \cdots (15)$$

where the latter, approximate, form applies when the wing is thin, i.e. $\varepsilon << 1$.

The/

The flow pattern is to include two contra-rotating point vortices, connected by cuts (which are not necessarily straight, as has been pointed out in Ref. 5) to the wing leading edges; one of strength γ anticlockwise at $\sigma = \sigma_o$ joined to the right-hand leading edge $\sigma = +s$ and one of strength $-\gamma$ at $\sigma = -\bar{\sigma}_o$ joined by a cut to $\sigma = -s$, if we assume port and starboard symmetry.

These vortices are subject to the Brown and Michael condition for zero net force on each vortex together with its cut[2], which has the form, in our present notation:

$$\left(\frac{\partial W_1}{\partial \sigma} \right)_{\sigma \to \sigma_o} = KU \left(\frac{2\,\bar{\sigma}_o}{s} - 1 \right), \qquad \cdots (16)$$

where W_1 is that part of W excluding the potential of the vortex at σ_o, i.e.

$$W_1 = W + \frac{i\gamma}{2\pi} \log (\sigma - \sigma_o). \qquad \cdots (17)$$

In addition the flow must separate from the section at the edges $\sigma = \pm s$, which means that $|\partial W/\partial \sigma|$ must be finite at these points.

We observe that, since there is no two-dimensional vortex sheet in the σ plane according to the Brown and Michael model, there is no singularity in the flow close to the leading edge to make the separation streamline there in line with the wing lower surface, as it should be. Instead, the separation streamline must form equal angles with the upper and lower surfaces at the edge. It therefore appears that for a wing with thickness, the Brown and Michael flow model is only really applicable when the wing is thin, as in the present treatment.

The conditions (7), (15) and (16) with the separation condition are sufficient to determine ϕ_h, or its equivalent, W. The flow in the σ plane is illustrated in Fig. 2.

3. Approximate Conformal Transformation of the Wing Cross-Sectional Profile

It is now required to transform the wing cross-sectional profile, given by equation (2), into a cut along the real axis, whilst keeping the distant parts of the plane unchanged.

If such a transformation is written as

$$\sigma_1 = \sigma + h(\sigma) \qquad \cdots (18)$$

then h must have the properties

Im/

$$\left.\begin{aligned} \mathrm{Im}\, h(y \pm i\,t\,T) &= \mp t\,T\,, \quad -s < y < s \\ \mathrm{Im}\, h(y) &= 0 \quad , \ |y| > s \\ \lim_{|\sigma| \to \infty} h(\sigma) &= 0 \quad . \end{aligned}\right\} \qquad \cdots (19)$$

Evidently the properties required for σ_1 are the same as for the complex potential of an acyclic flow past the cross-section profile in the σ plane, which, at great distances, becomes a uniform stream, parallel to Oy, with unit velocity.

For a general shape of thin section this potential may be found approximately by distributing sources of strength proportional to the local rate of change of section thickness along the "chord line", that is the real axis between $y = -s$ and $y = +s$, in the manner of thin aerofoil theory. The result is

$$\left.\begin{aligned} \sigma_1 &= \sigma + \frac{\varepsilon}{\pi} \int_{-s}^{s} T'\left(\frac{y'}{s}\right) \log\,(\sigma - y')\, dy' + O(K\varepsilon^2) \end{aligned}\right\}$$

so that

$$\left.\begin{aligned} h(\sigma) &\approx \frac{\varepsilon}{\pi} \int_{-s}^{s} T'\left(\frac{y'}{s}\right) \log(\sigma - y')\, dy' \\ &= \frac{\varepsilon\, s}{\pi} \int_{-s}^{s} \frac{T(y'/s)}{\sigma - y'}\, dy' \quad , \end{aligned}\right\} \qquad \cdots (20)$$

where (3) has been used.

It may be verified that h as given by (20) satisfies the first condition in (19) to the approximation shown and that the other two conditions are satisfied exactly. Henceforth, the symbol h will mean the approximate form given in (20).

The first two derivatives of h are needed later and these are given by

$$\left.\begin{aligned} h'(\sigma) &= \frac{\varepsilon}{\pi} \int_{-s}^{s} \frac{T'(y'/s)}{\sigma - y'}\, dy' \\ \text{and} \qquad h''(\sigma) &= -\frac{\varepsilon}{\pi} \int_{-s}^{s} \frac{T'(y'/s)}{(\sigma - y')^2}\, dy' \quad , \end{aligned}\right\} \qquad \cdots (21)$$

where the generalised principal value[9] is implied in the second equation. We see that, normally, h is $O(K\varepsilon)$, h' is $O(\varepsilon)$ and h'' is $O(\varepsilon/K)$.

Now/

Now although the expression for h is valid everywhere to first order if the section geometry is as specified earlier, the expression for h' is logarithmically singular at the section edges or at the spanwise position of any sharp corner of the cross section, so that it is invalid within a distance $O(e^{-1/\varepsilon})$ of such a corner, whilst the expression for h'' is invalid within a distance $O(\varepsilon)$ of edges or corners. Further differentiations increase the severity of the singularity.

To show the form of the singularities of h' at the edges $\sigma = \pm s$, for example, we write the first equation of (21) in the form

$$h'(\sigma) = \frac{\varepsilon}{\pi}\int_{-s}^{s}\left[T'\left(\frac{y'}{s}\right) - \frac{\sigma+s}{2s}\,T'(1) + \frac{\sigma-s}{2s}\,T'(-1)\right]\frac{dy'}{\sigma-y'}$$

$$+ \frac{\varepsilon}{\pi}\left[T'(1) - T'(-1)\right]\left(\frac{\sigma+s}{2s}\log\frac{\sigma+s}{2s} - \frac{\sigma-s}{2s}\log\frac{\sigma-s}{2s}\right)$$

$$+ \frac{\varepsilon}{\pi}\left[T'(-1)\log\frac{\sigma+s}{2s} - T'(1)\log\frac{\sigma-s}{2s}\right]. \qquad \cdots (22)$$

The first two terms on the right-hand side remain finite as $\sigma \to \pm s$, so that the last term gives the singularities of h' at $\sigma = \pm s$.

Calculations of vortex-core position described later seem, however, to be affected by these singularities only extremely close to the edges. For practical purposes the gap between the valid portion of the curve and the edge itself, (which is known to be the ultimate position of the core at zero incidence) is readily bridged by interpolation and so, in these calculations, the singularities have been ignored.

However, if surface pressures are to be calculated from the present solution, as has been done in Ref. 10, the singularities do cause difficulty and techniques such as those described by Van Dyke[11] must be used to find expressions valid, to first order in ε, right up to the edges or other corners.

4. Solution for the Slender-Body Potential

The transformation (18) now renders the slender-body problem as posed in the σ plane at the end of Section 2, into a simpler one in the σ_1 plane, which is illustrated in Fig. 3.

We are now required to solve for the flow past a flat plate in the σ_1 plane which is at right-angles to an initially uniform stream and has an appropriate pair of contra-rotating vortices, which are of the same strength as in the σ plane because the transformation (18) is conformal at the points $\sigma = \sigma_0$, $\sigma = -\bar{\sigma}_0$ (corresponding, respectively, to $\sigma_1 = \sigma_{0_1}$ and $\sigma_1 = -\bar{\sigma}_{0_1}$).

There/

There are to be equal and opposite values of outward normal velocity on the top and bottom of the plate with values which, from (15) and (18), are equal to

$$\frac{\partial \phi_h}{\partial \nu} \left| \frac{\partial \sigma}{\partial \sigma_1} \right| = U\varepsilon \left(KT - \frac{y}{x} T' \right) + O(K\varepsilon^2) \qquad \cdots (23)$$

at a point on the plate in the σ_1 plane corresponding to position y on the wing in the σ plane.

If the potential in the σ_1 plane is given by

$$\phi_{h_1} = \mathrm{Re}\, \Omega(\sigma_1) \qquad \cdots (24)$$

then, as σ and σ_1 become identical at great distances (equation (19)), the condition (7) becomes in the σ_1 plane

$$\lim_{|\sigma_1| \to \infty} \left(\phi_{h_1} - U\alpha z_1 - \frac{US'(x)}{2\pi} \log \sqrt{y_1^2 + z_1^2} \right) = 0, \qquad \cdots (25)$$

σ_1 being equal to $y_1 + iz_1$.

The separation condition in the σ plane must, in the absence of a vortex sheet, correspond to a simple separation from the plate edges in the σ_1 plane so the value of $|\partial\Omega/\partial\sigma_1|$ must be finite at $\sigma_1 = \pm s_1$, the wing-edge positions in the σ_1 plane.

Finally, the Brown and Michael force condition (equation (16)), may be easily evaluated in terms of Ω.

Evidently, the problem as now posed in the σ_1 plane is exactly the same as Brown and Michael's with the addition of the discontinuity of normal velocity across the wing "cut", which can be obtained by a source distribution on the cut of strength

$$m(y_1) = 2 \left(\frac{\partial \phi_h}{\partial \nu} \left| \frac{\partial \sigma}{\partial \sigma_1} \right| \right)$$

$$= 2U\varepsilon \left(KT - \frac{y}{x} T' \right) + O(K\varepsilon^2), \qquad \cdots (26)$$

where y_1 is the position on the cut corresponding to the spanwise position y on the wing cross section.

We therefore write

$$\Omega(\sigma_1) = \Omega_0(\sigma_1) + \omega(\sigma_1) \qquad \cdots (27)$$

where/

where Ω_0 is the potential of the sources and ω is exactly of the same form as Brown and Michael's solution (equation (7) of their paper) but contains cross-sectional effects because of equation (18), which relates σ_1 to the "physical" σ plane.

$$W_0(\sigma) = \Omega_0(\sigma_1) \qquad \cdots (28)$$

is seen to be the part of $W(\sigma)$ which is present at zero incidence and

$$w(\sigma) = \omega(\sigma_1) \qquad \cdots (29)$$

represents the effect of incidence.

We now have

$$\Omega_0(\sigma_1) = \frac{1}{2\pi}\int_{-s_1}^{s_1} m(y_1')\log(\sigma_1 - y_1')\,dy_1' \qquad \cdots (30)$$

and

$$\omega(\sigma_1) = -\frac{iy}{2\pi}\log\left(\frac{\sqrt{\sigma_1^2 - s_1^2} - \sqrt{\sigma_{0_1}^2 - s_1^2}}{\sqrt{\sigma_1^2 - s_1^2} + \sqrt{\bar{\sigma}_{0_1}^2 - s_1^2}}\right) - iU\alpha\sqrt{\sigma_1^2 - s_1^2}\,. \qquad \cdots (31)$$

It is readily verified that in view of (30) and (31), (27) satisfies the condition (25). Both w and W_0 are of the form (11) and satisfy (12).

5. Application of the Condition for Separation and Brown and Michael's Force Condition

Since the potential $W_0(\sigma)$ represents a velocity field with symmetry about the y axis it cannot affect the condition for separation, which is really one imposing local symmetry about the y axis at the tips $\sigma = \pm s$. The fact that the expression we derive below for $\partial W_0/\partial\sigma$, using our approximations to the source strength etc., exhibits a singularity at the tips is irrelevant to the above argument, since this is not true of the correct "inner" solution valid near the tips.

Thus, in the σ_1 plane, only $\omega(\sigma_1)$ is involved in this condition, which must therefore be of exactly the same form there as Brown and Michael's equation (8), so that it becomes, in our case

$$\frac{2\pi U\alpha}{\gamma} = \frac{1}{\sqrt{\sigma_{0_1}^2 - s_1^2}} + \frac{1}{\sqrt{\bar{\sigma}_{0_1}^2 - s_1^2}}\,. \qquad \cdots (32)$$

Cross-sectional effects are again present by virtue of equation (18). (32) shows that γ is $O(\alpha K)$, i.e. $O(K^2)$ at most.

To/

To apply the force condition (16) we require the quantity $(\partial W_1/\partial\sigma)_{\sigma\to\sigma_o}$.

Using (17) and (27)

$$\frac{\partial W_1}{\partial\sigma} = \frac{\partial W}{\partial\sigma} + \frac{iy}{2\pi(\sigma-\sigma_o)}$$

$$= \left(\frac{\partial\Omega_o}{\partial\sigma_1} + \frac{\partial\omega}{\partial\sigma_1} + \frac{iy}{2\pi(\sigma_1-\sigma_{o_1})}\right)\frac{\partial\sigma_1}{\partial\sigma}$$

$$+ \frac{iy}{2\pi}\left(\frac{1}{\sigma-\sigma_o} - \frac{1}{\sigma_1-\sigma_{o_1}}\frac{\partial\sigma_1}{\partial\sigma}\right). \qquad \cdots (33)$$

From (30) and (26)

$$\frac{\partial\Omega_o}{\partial\sigma_1} = \frac{1}{2\pi}\int_{-s_1}^{s_1}\frac{m(y_1')}{\sigma_1-y_1'}\,dy_1'$$

$$= \frac{1}{2\pi}\int_{-s}^{s}\frac{2U\varepsilon\,[KT(y'/s) - K\,y'/s\,T'(y'/s)]\,dy'}{\sigma-y'}$$

$$+ O(K\varepsilon^2)$$

$$= \frac{KU\varepsilon}{\pi}\int_{-s}^{s}\left\{\frac{T(y'/s)}{\sigma-y'} + \frac{1}{s}T'(y'/s)\right.$$

$$\left. - \frac{\sigma}{s}\frac{T'(y'/s)}{\sigma-y'}\right\}dy' + O(K\varepsilon^2)$$

$$= \frac{KU}{s}\left\{h(\sigma) - \sigma h'(\sigma)\right\} + O(K\varepsilon^2), \qquad \cdots (34)$$

where use has been made of (3), (20) and (21).

From/

From (31) and (32)

$$\frac{\partial\omega}{\partial\sigma_1} = \frac{iy}{2\pi}\left(\frac{\sigma_1}{\sigma_1^2 - s_1^2 + \sqrt{(\sigma_1^2 - s_1^2)(\bar{\sigma}_{o_1}^2 - s_1^2)}} \right.$$

$$- \frac{\sigma_1}{\sigma_1^2 - s_1^2 - \sqrt{(\sigma_1^2 - s_1^2)(\sigma_{o_1}^2 - s_1^2)}}$$

$$\left. - \frac{\sigma_1}{\sqrt{(\sigma_1^2 - s_1^2)(\sigma_{o_1}^2 - s_1^2)}} - \frac{\sigma_1}{\sqrt{(\sigma_1^2 - s_1^2)(\bar{\sigma}_{o_1}^2 - s_1^2)}} \right) . \quad \cdots (35)$$

(34) and (35) may be inserted in (33) and the limit of the bracket which multiplies $\partial\sigma_1/\partial\sigma$ found with little difficulty. The last term shown in (33), however, requires some care to obtain the limit. Thus, using L'Hospital's rule

$$\lim_{\sigma \to \sigma_o} \left(\frac{1}{\sigma - \sigma_o} - \frac{1}{\sigma_1 - \sigma_{o_1}} \frac{\partial\sigma_1}{\partial\sigma} \right) = \lim_{\sigma \to \sigma_o} \left(\frac{-(\sigma - \sigma_o)\dfrac{\partial^2\sigma_1}{\partial\sigma^2}}{\sigma_1 - \sigma_{o_1} + (\sigma - \sigma_o)\dfrac{\partial\sigma_1}{\partial\sigma}} \right)$$

$$= -\frac{1}{2} \left\{ \frac{\dfrac{\partial^2\sigma_1}{\partial\sigma^2}}{\dfrac{\partial\sigma_1}{\partial\sigma}} \right\}_{\sigma = \sigma_o}$$

$$= -\tfrac{1}{2} h''(\sigma_o) + O(\varepsilon^2/K) . \quad \cdots (36)$$

If (16) is first multiplied throughout by

$$\left(\frac{\partial\sigma_1}{\partial\sigma} \right)^{-1}_{\sigma = \sigma_o} = 1 - h'(\sigma_o) + O(\varepsilon^2)$$

and the above substitutions are made, we find the result

$$\frac{iy}{2\pi}$$

$$\frac{iy}{2\pi}\left\{\frac{\sigma_{o_1}}{\sigma_{o_1}^2 - s_1^2 + \sqrt{(\sigma_{o_1}^2 - s_1^2)(\bar{\sigma}_{o_1}^2 - s_1^2)}} - \frac{\sigma_{o_1}}{\sqrt{(\sigma_{o_1}^2 - s_1^2)(\bar{\sigma}_{o_1}^2 - s_1^2)}}\right.$$

$$\left. - \frac{\sigma_{o_1}}{\sigma_{o_1}^2 - s_1^2} + \frac{s_1^2}{2\sigma_{o_1}(\sigma_{o_1}^2 - s_1^2)} - \frac{h''(\sigma_o)}{2}\right\}$$

$$= \frac{KU}{s}\left\{2\bar{\sigma}_o - s - h(\sigma_o) + h'(\sigma_o)(s + \sigma_o - 2\bar{\sigma}_o)\right\} + O(K\varepsilon^2)\ . \qquad \cdots (37)$$

The first four terms in the bracket on the left-hand side may now be regarded as a function of the three variables

$$\left.\begin{aligned} s_1 &= s + h(s) \\ \sigma_{o_1} &= \sigma_o + h(\sigma_o) \\ \text{and} \quad \bar{\sigma}_{o_1} &= \bar{\sigma}_o + h(\bar{\sigma}_o)\ , \end{aligned}\right\} \qquad \cdots (38)$$

where, in the last equation, we have used the fact, which can be deduced from (20), that

$$\bar{h}(\bar{\sigma}_o) \equiv h(\bar{\sigma}_o). \qquad \cdots (39)$$

Expansion of this function as far as the linear terms yields, with the same error as in (37):

$$\frac{iy}{2\pi}\left\{A_0 + A_1 h(\sigma_o) + A_2 h(\bar{\sigma}_o) + A_3 h(s) - \frac{h''(\sigma_o)}{2}\right\}$$

$$= \frac{KU}{s}\left\{2\bar{\sigma}_o - s - h(\sigma_o) + h'(\sigma_o)(s + \sigma_o - 2\bar{\sigma}_o)\right\} + O(K\varepsilon^2), \qquad \cdots (40)$$

where

A_o/

$$A_0 = \frac{\sigma_0}{\sigma_0^2 - s^2 + \sqrt{(\sigma_0^2 - s^2)(\bar{\sigma}_0^2 - s^2)}} - \frac{\sigma_0}{\sqrt{(\sigma_0^2 - s^2)(\bar{\sigma}_0^2 - s^2)}} - \frac{\sigma_0}{\sigma_0^2 - s^2} + \frac{s^2}{2\sigma_0(\sigma_0^2 - s^2)}$$

$$A_1 = \left(\frac{s^2}{\sqrt{(\sigma_0^2 - s^2)(\bar{\sigma}_0^2 - s^2)}} - 1 \right) \left(\frac{1}{\sqrt{\sigma_0^2 - s^2} + \sqrt{\bar{\sigma}_0^2 - s^2}} \right)^2 + \frac{\sigma_0^2}{(\sigma_0^2 - s^2)^2} - \frac{s^2}{2\sigma_0^2(\sigma_0^2 - s^2)}$$

$$A_2 = \frac{\sigma_0 \bar{\sigma}_0}{\sqrt{(\sigma_0^2 - s^2)(\bar{\sigma}_0^2 - s^2)}} \left\{ \frac{1}{\bar{\sigma}_0^2 - s^2} - \left(\frac{1}{\sqrt{\sigma_0^2 - s^2} + \sqrt{\bar{\sigma}_0^2 - s^2}} \right)^2 \right\}$$

and

$$A_3 = - \frac{s\sigma_0}{(\sigma_0^2 - s^2)^2} \left\{ 1 + \left(\frac{\sigma_0^2 - s^2}{\bar{\sigma}_0^2 - s^2} \right)^{3/2} \right\} \qquad \cdots (41)$$

Equation (40) yields two equations for the vortex co-ordinates, y_0 and z_0 (the real and imaginary parts of σ_0, respectively) when real and imaginary parts are taken. These are solved numerically by the method of Brown and Michael[2] which consists of adjusting y_0 for a fixed z_0 until two values of the ratio $\gamma/2\pi KUs$ derived from the two equations, are as close to each other as required. The corresponding value of α/K is then calculated from an expansion of (32) in the form

$$\frac{\alpha}{K} = \frac{\gamma}{2\pi KUs} \left\{ \mathrm{Re} \frac{2s}{\sqrt{\sigma_0^2 - s^2}} - \mathrm{Re} \frac{2s\sigma_0}{(\sigma_0^2 - s^2)^{3/2}} \cdot \mathrm{Re}\, h(\sigma_0) \right.$$

$$\left. + \mathrm{Im} \frac{2s\sigma_0}{(\sigma_0^2 - s^2)^{3/2}} \cdot \mathrm{Im}\, h(\sigma_0) + \mathrm{Re} \frac{2s^2}{(\sigma_0^2 - s^2)^{3/2}} \cdot h(s) \right\} + O(\varepsilon^2), \qquad \cdots (42)$$

$h(s)$ being entirely real.

When the function h is zero, equations (40) and (42) reduce, respectively, to equations (11) and (8) of Ref. 2.

6. Normal-Force Coefficient

The normal-force coefficient may be evaluated from the pressure distribution (see Ref. 10), or by application of the momentum theorem as in Ward's general slender body method[8], the latter leading to a contour integral which yields the result

$$\frac{C_N}{K^2}$$

$$\frac{C_N}{K^2} = \frac{\alpha}{K}\left(\frac{4\pi}{s^2}\sqrt{\sigma_{o_1}^2 - s_1^2}\sqrt{\bar{\sigma}_{o_1}^2 - s_1^2} - \frac{S'}{sK} - \frac{2S}{s^2} + 2\pi\frac{s_1^2}{s^2}\right). \quad \cdots (43)$$

The pressure distribution method, as given in Ref. 10, yields substantially the same results as equation (43) in the case of the rhombic cross section, (see below), even though the singularities in pressure at the edges have there been removed in the manner of Ref. 11, as previously mentioned.

7. Comparison of the Theory with Experiment for Wings of Rhombic Cross-Section

If the delta wing being considered has cross-sections which are similar rhombuses, then the equation for T is

$$T\left(\frac{y}{s}\right) = 1 - \left|\frac{y}{s}\right|, \quad \cdots (44)$$

so that, from equation (20), we have

$$h(\sigma) = \frac{2s\varepsilon}{\pi}\left(\frac{\sigma+s}{2s}\log\frac{\sigma+s}{2s} + \frac{\sigma-s}{2s}\log\frac{\sigma-s}{2s} - \frac{\sigma}{s}\log\frac{\sigma}{2s}\right). \quad \cdots (45)$$

Hence

$$h'(\sigma) = \frac{\varepsilon}{\pi}\left(\log\frac{\sigma+s}{2s} + \log\frac{\sigma-s}{2s} - 2\log\frac{\sigma}{2s}\right) \quad \cdots (46)$$

and

$$h''(\sigma) = \frac{\varepsilon}{\pi}\left(\frac{1}{\sigma+s} + \frac{1}{\sigma-s} - \frac{2}{\sigma}\right). \quad \cdots (47)$$

Equation (43) becomes

$$\frac{C_N}{K^2} = \frac{\alpha}{K}\left(\frac{4\pi}{s^2}\sqrt{\sigma_{o_1}^2 - s_1^2}\sqrt{\bar{\sigma}_{o_1}^2 - s_1^2} - 8\varepsilon + 2\pi\frac{s_1^2}{s^2}\right). \quad \cdots (48)$$

These equations have been used to evaluate the vortex-core position and C_N/K^2, as described above, over a range of α/K, for three values of ε, corresponding to three experimental models. The values of ε were 0·031, 0·176 and 0·268 (the corresponding wings being respectively

referred/

referred to as models 031, 176 and 268 on the accompanying graphs). Results for $\varepsilon = 0$ were also found, so that they could be checked against those of Brown and Michael[2] and this check proved entirely satisfactory. (N.B. In Fig. 4 theoretical results are also shown for $\varepsilon = 0{\cdot}088$, corresponding to a proposed fourth model which was not tested owing to lack of time).

The models were each 23 inches long with a leading edge sweepback of 80° (corresponding to $K = 0{\cdot}176$) and they were tested over a suitable range of values of α/K at a speed of about 60 ft sec^{-1} in the 2·75 ft × 3·75 ft low-speed wind tunnel at the University of Salford, Department of Mechanical Engineering.

The vortex-core positions were defined as positions of minimum total head and were found using a remotely-controlled, five-tube probe. Surface pressures were also measured on one of the four faces of the rhombic-cross-sectioned wing, use being made of the wing symmetry to obtain upper and lower surface pressures from the same tappings. Near the sharp leading edges, pressures were measured by cutting a shallow groove in the surface which was connected at its inboard end to a tube which passed out of the model in the normal way. This groove was covered with thin adhesive tape which was pierced, using a jig, at the desired pressure measuring station. Surface flow patterns established that the tape did not seriously affect the flow, that the boundary layer was laminar at the secondary separation and also that the flow was effectively conical over at least 70% of the model length from the apex. All flow surveys and pressure measurements were made at the 60% station. Full details of the models and the experiments are given in Ref. 10.

In Fig. 4 theoretical and experimentally-found, vortex-core positions are plotted along with Smith's theoretical results for a flat plate (Ref. 4). Because the number of experimental points was so low (3 per incidence) results obtained from other sources have been superimposed.

Fink and Taylor (Ref. 12) used a model of aspect ratio 0·705 having a flat upper surface and a lower surface with a constant chamfer parallel to the leading edge. In the plane where the cores were examined (41·7% root chord) the cross-section was a truncated triangle, but from the apex to 36% chord the section was an isosceles triangle with an edge angle of 4·75°. It is reasonable to assume that the vortices formed at the traversing section will not be very different from those which would be found if the wing was conical up to the traversing section. Further, Maskell (Ref. 15) has suggested and Kirkpatrick (Ref. 13) has demonstrated that a change of a few degrees in the anhedral of the leading-edge bisector would not greatly affect the position of the vortices relative to axes in the direction of the leading-edge bisector and normal to this. For the purposes of this paper these rotated axes have been taken as the y, z axes. The model of Ref. 12 can therefore be identified with $\varepsilon = 0{\cdot}041$. The core centre was again found as the point of total-head minimum, using a Kiel tube. Core positions corresponding to specific values of α/K were interpolated from the published results.

Kirkpatrick and Kirkpatrick and Field (Refs. 13 and 14) also used a Kiel tube in their investigations of rhombic-cross-sectioned wings, which included models with ε equal to 0·132 and 0·268. The core position was estimated from the total head values of three selected points in the neighbourhood of the vortex core, assuming the total-head contours to be

circular./

circular. There seems to be a consistent and significant difference in the results for $\varepsilon = 0{\cdot}268$ as found in Ref. 14 and the present tests. These differences may possibly be due to a slight yaw angle being present in the rigging of either the model of Ref. 14 or in that of the present model, or in both, but with different magnitudes.

It can be seen that the vertical distance of the vortex core above the wing surface found experimentally on the thinnest model tested agrees well with both Smith (Ref. 4) and the present theoretical predictions for $\varepsilon = 0$ (which corresponds to the results of Brown and Michael (Ref. 2)). However, the spanwise position of the core is much more inboard than Ref. 2 suggests and slightly more inboard than Ref. 4. The present theory predicts fairly well the spanwise vortex shift due to thickness, but totally fails to account for the vertical core movements. At low α/K values (about $0{\cdot}5$) this vertical shift is almost equal to the spanwise movement and at higher α/K values it can be twice as much. However, the normal-force coefficients shown on Fig. 5 show the same variations due to thickness as the present theory suggests.

References/

References

No.	Author(s)	Title, etc.
1	R. Legendre	Écoulement au Voisinage De La Pointe Avant D'une Aile A Forte Fleche Aux Incidences Moyennes. La Recherche Aeronautique, No. 30, 1952, No. 31, 1953, and No. 35, 1953.
2	C. E. Brown and W. H. Michael	Effect of Leading-Edge Separation on the Lift of a Delta Wing. J. Aero. Sciences, Vol. 21, pp 690-695 and 706, 1954.
3	K. W. Mangler and J. H. B. Smith	A Theory of the Flow Past a Slender Delta Wing with Leading-Edge Separation. Proc. Roy. Soc. A, Vol. 251, pp 220-217, 1959.
4	J. H. B. Smith	Improved Calculation of Leading-Edge Separation from Slender Delta Wings. Proc. Roy. Soc. A, Vol. 306, pp 67-90, 1968.
5	J. H. B. Smith	A Theory of the Separated Flow from the Curved Leading Edge of a Slender Wing. R. & M.3116, 1959.
6	C. E. Jobe	An Aerodynamic Theory of Slender Wings with Leading-Edge Separation. M.Sc. Thesis, Ohio State University, 1966.
7	J. H. B. Smith	The Effect of Wing Thickness on Leading-Edge Separation from Slender Delta Wings. 8th Symposium of Advanced Problems in Fluid Mechanics, Tarda, Poland, 1967.
8	G. N. Ward	Linearized Theory of Steady High-Speed Flow, Part 3. Cambridge University Press, 1955.
9	W. R. Sears (Ed.)	General Theory of High-Speed Aerodynamics. (High-Speed Aerodynamics and Jet Propulsion Series, Vol. VI.) p 233, Oxford University Press, 1955.
10	S. C. Russell	The Effect of Conical Thickness on the Flow about Low-Aspect-Ratio Wings with Sharp Leading Edges. Ph.D. Thesis, University of Salford, 1969.

11/

References (continued)

No.	Author(s)	Title, etc.
11	M. Van Dyke	Perturbation Methods in Fluid Mechanics. (Applied Mathematics and Mechanics Series, Vol. 8), Academic Press, 1964.
12	P. T. Fink and J. Taylor	Some Low-Speed Experiments with a 20° Delta Wing. R. & M. 3489, 1966.
13	D. L. I. Kirkpatrick	Experimental Demonstration of the Similarity of Leading-Edge Vortices above Slender Wings in Subsonic Conical Flow. Jahrbuch 1967 der W.G.L.R.
14	D. L. I. Kirkpatrick and J. D. Field	Experimental Investigation of the Position of the Leading-Edge Vortices above Slender Delta Wings with Rhombic Cross Sections in Subsonic Conical Flow. R.A.E. T.R. 66068, March, 1966.
15	E. C. Maskell	Similarity Laws Governing the Initial Growth of Leading-Edge Vortex Sheets in Conical Flow past Sharp-Edged Slender Bodies. 10th International Congress of Applied Mechanics, Stresa, 1960.

BMG

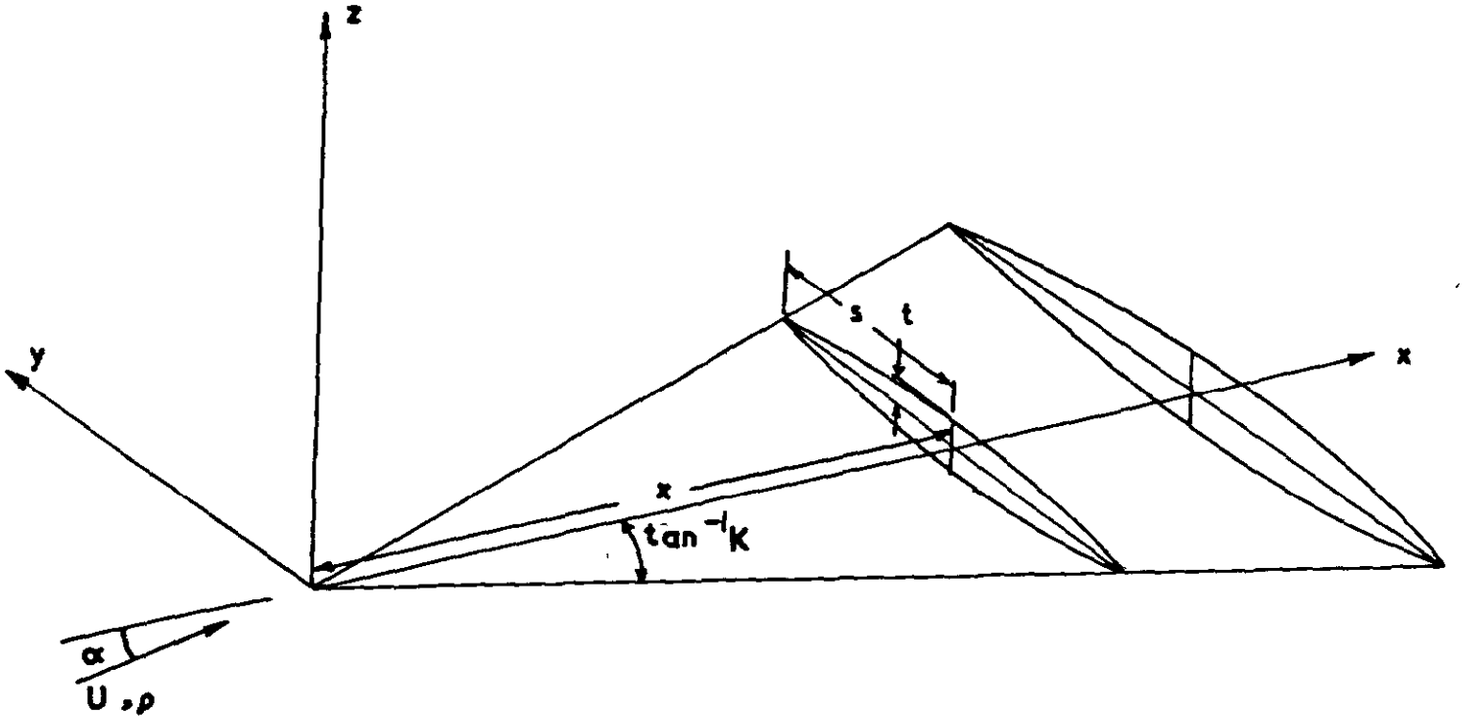

FIG. 1

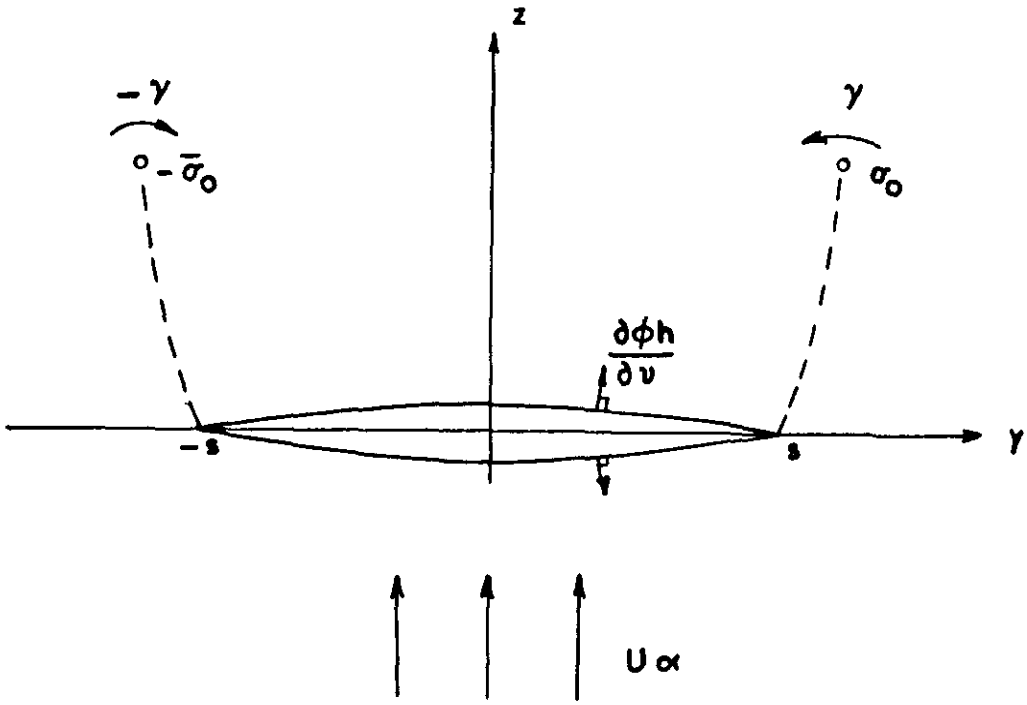

FIG.2 The σ plane

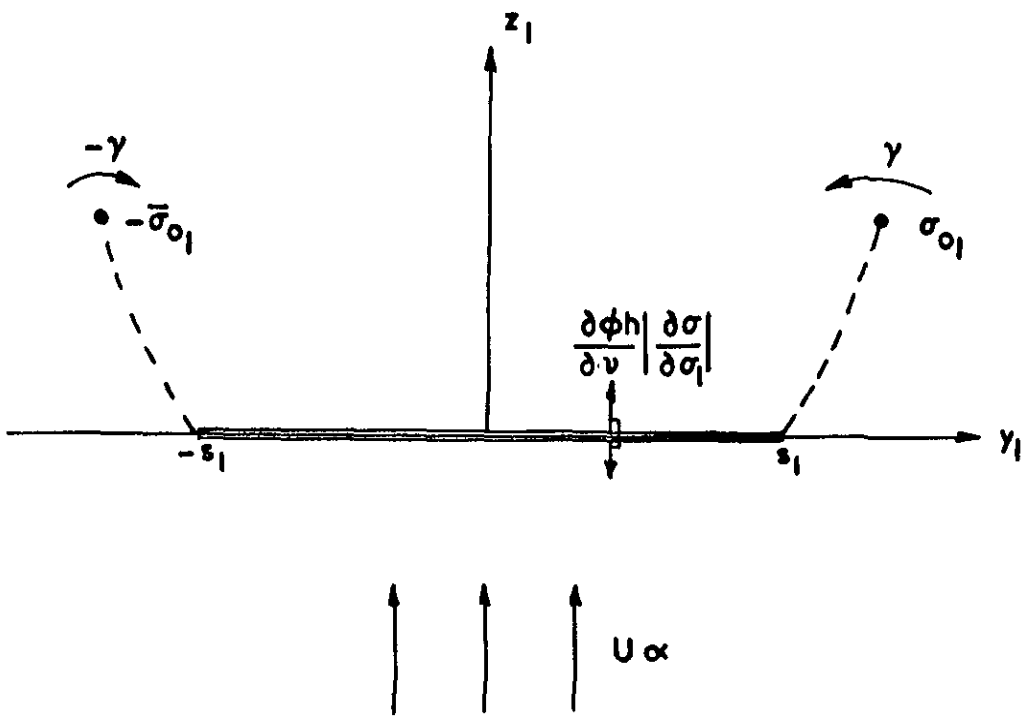

FIG.3 The σ_1 plane

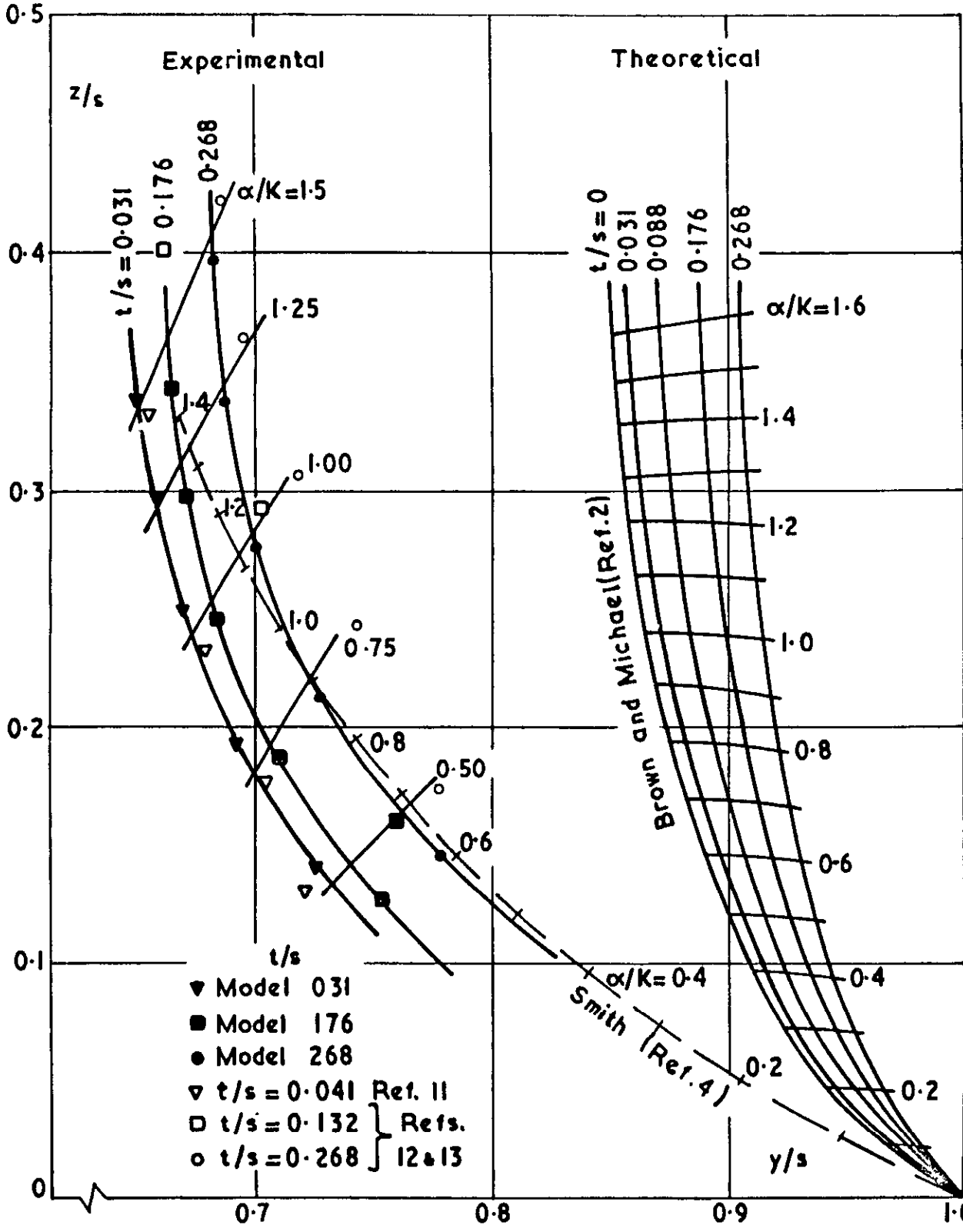

FIG. 4. Theoretical and experimental vortex core positions

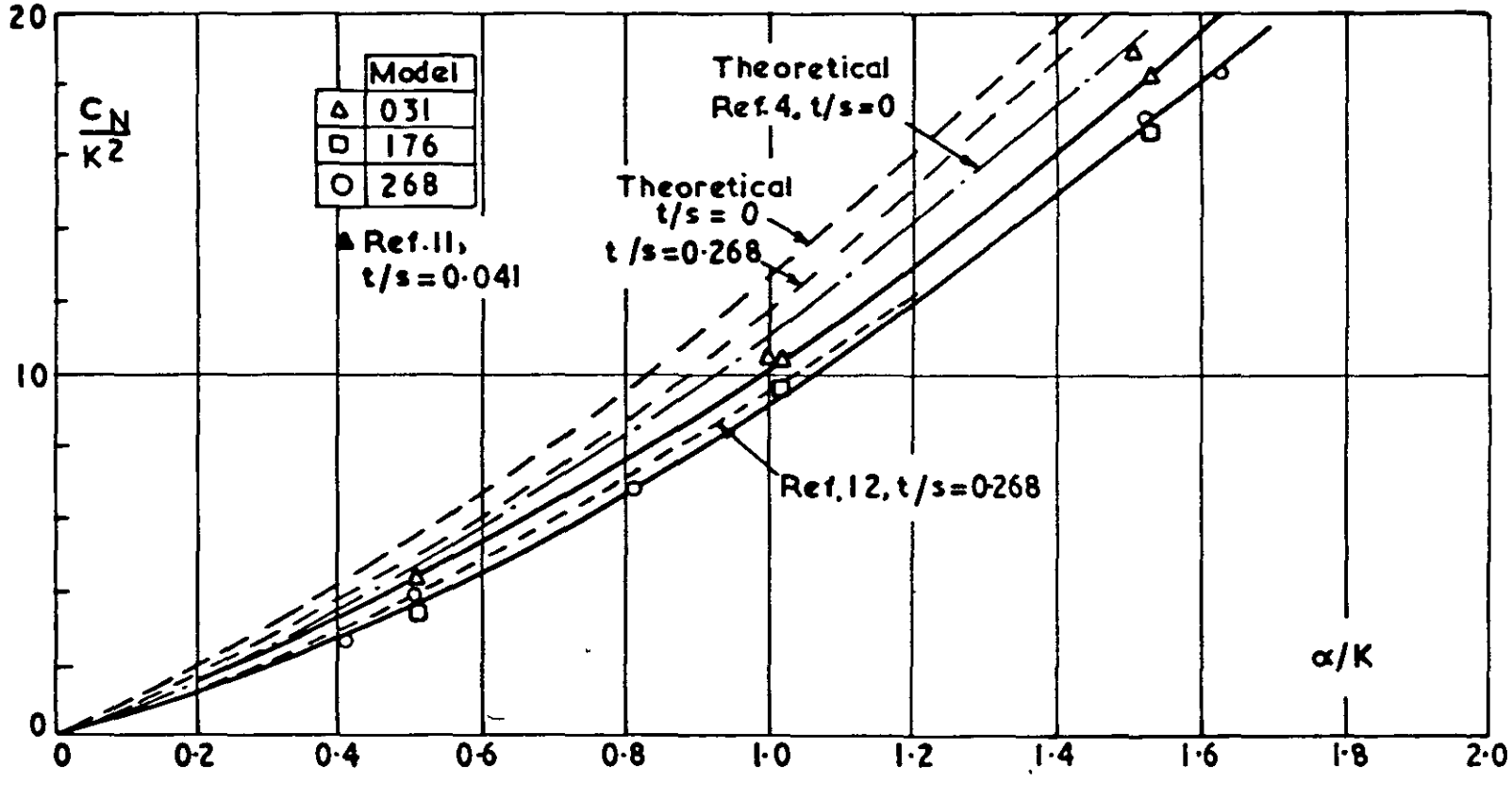

FIG.5 C_N/K^2 against α/K

A.R.C. C.P. No.1189
April, 1971
H. Portnoy and S. C. Russell

THE EFFECT OF SMALL CONICAL THICKNESS DISTRIBUTIONS ON THE SEPARATED FLOW PAST SLENDER DELTA WINGS

A method is described for calculating the effects of small conical distributions on the flow past slender delta wings with leading-edge separation, using the flow model of Brown and Michael. Comparisons with limited experimental results indicate that, despite the basic inaccuracies of the model, some of the effects of thickness are predicted adequately.

A.R.C. C.P. No.1189
April, 1971
H. Portnoy and S. C. Russell

THE EFFECT OF SMALL CONICAL THICKNESS DISTRIBUTIONS ON THE SEPARATED FLOW PAST SLENDER DELTA WINGS

A method is described for calculating the effects of small conical distributions on the flow past slender delta wings with leading-edge separation, using the flow model of Brown and Michael. Comparisons with limited experimental results indicate that, despite the basic inaccuracies of the model, some of the effects of thickness are predicted adequately.

A.R.C. C.P. No.1189
April, 1971
H. Portnoy and S. C. Russell

THE EFFECT OF SMALL CONICAL THICKNESS DISTRIBUTIONS ON THE SEPARATED FLOW PAST SLENDER DELTA WINGS

A method is described for calculating the effects of small conical distributions on the flow past slender delta wings with leading-edge separation, using the flow model of Brown and Michael. Comparisons with limited experimental results indicate that, despite the basic inaccuracies of the model, some of the effects of thickness are predicted adequately.

Produced and published by
HER MAJESTY S STATIONERY OFFICE
To be purchased from
49 High Holborn, London WC1V 6HB
13a Castle Street, Edinburgh EH2 3AR
109 St Mary Street, Cardiff CF1 1JW
Brazennose Street, Manchester M60 8AS
50 Fairfax Street, Bristol BS1 3DE
258 Broad Street, Birmingham B1 2HE
80 Chichester Street, Belfast BT1 4JY
or through booksellers

Printed in England

C.P. No. 1189

SBN 11 470457 0